LWT - Food Science and Technology 238 (2025) 118840



Contents lists available at ScienceDirect

LWT

journal homepage: www.elsevier.com/locate/lwt



Innovative cold plasma modification of *Caulerpa prolifera* proteins: A strategy to improve techno-functional and antioxidant properties

Aysun Yücetepe [a,b], Emine Şükran Okudan [c], Tuba Esatbeyoglu [b,*]

[a] Department of Food Engineering, Faculty of Engineering, Aksaray University, TR-68100, Aksaray, Turkey
[b] Department of Molecular Food Chemistry and Food Development, Institute of Food and One Health, Gottfried Wilhelm Leibniz University Hannover, Am Kleinen Felde 30, 30167, Hannover, Germany
[c] Faculty of Fisheries, Akdeniz University, Dumlupınar Bulvarı, 07058, Antalya, Turkey

ARTICLE INFO

Keywords:
Non-thermal technique
Macroalgae
Protein
Protein functionality
Protein secondary structure

ABSTRACT

In this study, the effects of cold plasma (CP) on structural, techno-functional, and antioxidant properties of *Caulerpa prolifera* proteins were investigated for the first time. *C. prolifera* proteins were modified by CP to improve their techno-functional and antioxidant properties. CP conditions (power: 5, 47.5, 90 W; treatment time: 1, 15.5, 30 min; pressure: 30, 60, 90 Pa) were optimized to determine the effect of CP on water absorption capacity (WAC),oil absorption capacity (OAC), emulsion activity (EA), emulsion stability (ES), foaming capacity (FC), foaming stability (FS), free sulfhydryl group (SH) content, protein solubility (PS), and antioxidant activity (AOA) of the proteins extracts and functional groups, microstructure, color, and nutritional properties of the modified proteins were investigated. Optimum conditions were 87.50 W power, 6.63 min treatment time, and 90 Pa pressure. At optimum conditions, WAC, OAC, EC, ES, FC, FS, Free-SH content, AOA_{DPPH}, AOA_{CUPRAC}, and PS were 232.04 ± 10.25 g/hg, 350.66 ± 15.78 g/hg, 49.50 ± 5.05 g/hg, 49.95 ± 0.51 g/hg, 101.26 ± 7.89 g/hg, 70.10 ± 2.85 g/hg, 18.28 ± 1.50 mmol/kg, 3.78 ± 0.40 g Trolox equivalent (TE)/kg, 8.31 ± 0.01 g TE/kg, and 22.30 ± 4.02 g/hg, respectively. The findings showed that CP provided an increase in WAC, AOA, and PS of proteins and the results were confirmed by investigating changes in secondary structure of proteins.

1. Introduction

Proteins play a crucial functional role on maintaining the stability and quality of food. Functional properties of proteins include i) solubility and water absorption capacity by hydration, ii) emulsification and foaming properties by surface properties such as hydrophobicity, hydrophilicity, or surface charges, and iii) gelatinization and foaming properties determined by its amino acid sequence, composition, or size (Wang, Fu, Wang, & Zhang, 2022). Moreover, extraction method applied and/or the processes applied after extraction affect the functional properties of proteins. For instance, a decrease in surface hydrophobicity and an increase in surface water dispersion are factors that contribute most to high-water absorption capacity (Basak and Annapure, 2022).

Non-thermal techniques such as cold plasma (CP) can enhance the potential of the usage of proteins as food additives in food industry by improving nutritional, bioactive, and techno-functional properties of foods (Barbhuiya et al., 2021). CP is described as energy efficient, low-cost, sustainable, and a "green" method due to less use of solvents and chemicals (N. Misra & Roopesh, 2019). CP application, a non-equilibrium atmospheric discharge, contains the first stage of plasma production consists of ionization, dissolution, and excitation steps. Secondary plasma processes include production of reactive oxygen and reactive nitrogen species (ROS and RNS) (Hara & Adachi, 2021). Plasma is the fourth state of matter produced from ionized gas that contains reactive oxygen species and nitrogen species, ultraviolet radiation, free radicals, and charged particles. It is generated when electrical energy is applied to gas molecules that are present or flowing between two electrodes having a high electrical potential difference; gas ionization results from free electrons colliding with gas molecules (Laroque et al., 2022). In CP, overall temperature of the gas remains low because cooling of the ions and uncharged molecules is more efficient than energy transfer from electrons (Y. Chen, Cheng, & Sun, 2020). The distribution and concentration of ROS and RNS can change depending on the discharge design, such as gliding arc discharge, radio-frequency plasma, or corona discharge, affecting their interaction with

* Corresponding author.
E-mail address: esatbeyoglu@foh.uni-hannover.de (T. Esatbeyoglu).

https://doi.org/10.1016/j.lwt.2025.118840
Received 28 August 2025; Received in revised form 29 November 2025; Accepted 29 November 2025
Available online 5 December 2025
0023-6438/© 2025 The Authors. Published by Elsevier Ltd. This is an open access article under the CC BY license (http://creativecommons.org/licenses/by/4.0/).

biomolecules. These reactive species can modify proteins, lipids, and nucleic acids through their interactions with biomolecules (Gavahian et al., 2018; Sharifian et al., 2019).

CP technique can be used in modification of proteins (N. Misra & Roopesh, 2019). For instance, in the study of P. Wang, Wang, Du, Han, & Yu (2024), improvements in techno-functional properties such as oil absorption capacity, foaming and emulsifying activity, and solubility occurred after soybean meal was treated by CP (P. Wang et al., 2024). Similarly, in the study of Ji et al. (2018), CP application resulted in a high-water absorption capacity and a decrease in surface hydrophobicity of peanut protein isolates due to increased surface area and hydrophilic groups. Also, partial unfolding and breakdown of protein aggregates can enhance interfacial activity and emulsifying ability. Electrostatic repulsions inside proteins are caused by the strong negative charge that plasma introduces, and this improves the stability and activity of emulsions (Mehr and Koocheki, 2020).

CP is increasingly applied not only in food processing but also in plant biostimulation, macroalgal bioprocessing, plasma-activated liquids, and biomedical/materials research (Gavahian et al., 2018; Sharifian et al., 2019). Plant physiological and biochemical properties which include germination rate, root growth, and photosynthetic efficiency, and antioxidant activity, can be improved by CP treatment, according to recent studies conducted by Perner and Matoušek (2024) and Wei et al. (2023). Moreover, CP has shown therapeutic potential in several medical applications, including cancer therapy, wound healing, dermatology, dentistry, and management of infection (Apelqvist et al., 2024; Dubey et al., 2022; Laroussi, 2020; Metelmann et al., 2018).

Macroalgae are a valuable source of proteins exhibiting important nutritional, bioactive, and techno-functional properties. Compared to other plant-based protein sources, macroalgae exhibit faster growth, lower water consumption, superior photosynthetic efficiency, and the capacity to store carbon (Sensu et al., 2023). The innovative aspects and novelty of the present study are addressed by finding alternative proteins from new protein sources such as macroalgae, modifying techno-functional and antioxidant properties, and assessing the potential of the proteins within food industry, thereby contributing to the development of healthier and sustainable foods/food ingredients. Additionally, this study explains the factors behind cold plasma-induced modifications in algae-based proteins techno-functional properties by understanding the changes occurring in secondary structure of the protein. To the best of our knowledge, there has not yet been any study on modification of protein extracts from *Caulerpa prolifera* macroalgae by CP application in terms of techno-functional properties and investigation-related structural changes. In the present study, techno-functional properties of *C. prolifera* protein extracts (CP-PE) were modified by using CP and process conditions were optimized by using Response Surface Methodology (RSM). Water/oil absorption capacity; emulsification, foaming, and solubility properties; free sulfhydryl group content; and antioxidant activity of the modified protein extracts were investigated. Characterization studies of the protein structure were carried out using Fourier Transform Infrared (FT-IR) spectroscopy and Scanning Electron Microscopy (SEM). In addition, color and nutritional properties were determined. This study is important because it demonstrates the potential of cold plasma treatment to improve techno-functional and antioxidant properties of macroalgae-based proteins as an alternative protein source, offering a novel and sustainable proteins with improved technological value for the food industry by using an innovative approach like cold plasma treatment.

2. Material and method

2.1. Material

Caulerpa prolifera was collected from Mediterranean coasts of Türkiye at coordinates of 36°27′40.47″N and 30°32′38.18″E (Fig. 1) and it was identified by Dr. Emine Şükran Okudan. The algae were cleaned and dried at 30 °C without direct exposure to sunlight. The powdered (<500 μm particle size) algae were packaged in an opaque polyethylene bag, sealed tightly to protect from oxygen and daylight exposure, and stored at −20 °C.



Fig. 1. *Caulerpa prolifera* photographed *in situ* by Dr. Emine Şükran Okudan.

2.2. Chemicals

2,2-Diphenyl-1-picrylhydrazyl (DPPH) and hydrochloric acid (12 mol/L) were purchased from Sigma-Aldrich (Steinheim, Germany) and Merck KGaA (Darmstadt, Germany). Acetonitrile (HPLC grade) and acetic acid (HPLC grade) were purchased from VWR International (Leuven, Belgium). Methanol was provided from Carl Roth (HPLC grade, Karlsruhe, Germany). 3-Meracptopropionic acid was purchased from Alfa Aesar (Massachusetts, USA). Bicinchoninic acid (BCA) protein assay kit was provided from Thermo Scientific (Rockford, USA). Hemicellulase was purchased from DSM (Koninklijke DSM N.V, Heerlen, Denmark). Amino acid standards of analytical grade were purchased from Sigma-Aldrich (Steinheim, Germany). Ultrapure water was prepared by Purelab® flex 3 from Elga Veolia (Celle, Germany), which was used for all sample preparations.

2.3. Ultrasound-assisted enzymatic protein extraction

Proteins from *Caulerpa prolifera* were extracted by using the method that was used in our previous study with some modifications (Yucetepe et al., 2022). The extracts were stored at −20 °C in the dark until further analysis.

2.4. Determination of protein content

Protein content (PC) of the protein extracts was determined using Bicinchoninic acid (BCA) method spectrophotometrically by a UV spectrophotometer (Sci-UV1000, Scilogex, Rocky Hill, Connecticut, USA), (Smith et al., 1985). Bovine serum albumin was used as the standard, and PC was expressed as grams per kilograms sample dry weight (dw).

2.5. Cold plasma application

CP treatments were carried out using a low-pressure cold plasma device with a capacity discharge configuration. The device includes 8 parallel stainless-steel electrodes, each 100 mm and symmetrically set in a rounded borosilicate glass chamber. The device (type Femto; Diener Electronic, Ebhausen, Germany) has a rotating chamber with rotary columns that guarantee uniform plasma exposure of protein extracts.

Rotating chamber of the device with 13.56 mHz, and 100 W maximum power are its unique features (Fig. 2). This arrangement was chosen to guarantee consistent exposure of the protein extracts to plasma. The distance between each electrode is 5-10 mm. The thickness of the dielectric layer is about 7-10 mm. Cold plasma was generated by using atmospheric air (~78 % N_2, 21 %O_2, 1 % other gases including CO_2, Ar) as the inducing gas at controlled low pressure (from 40 to 90 Pa). The rotary pump evacuates the gas with an input capacity of 6 m^3/h (Rotary pump, Pfeiffer, Asslar, Germany). Table 1 summarizes the application parameters (power, pressure, and treatment time). To increase the amount of contact surface with the plasma, 2 g of the freeze-dried protein extracts were uniformly applied as a thin layer (~2–3 mm thick) at the bottom of 200 mL square glass bottles. To expose the protein extracts to direct plasma, the caps of the bottles were removed and they were set on the revolving columns inside the chamber. The sample layer and the electrode surface were separated by a distance of 55 mm. All operations were carried out at 24 ± 2 °C. Reactive oxygen and nitrogen species may be efficiently generated and delivered with this technique, allowing for controlled changes of protein structure and function without excessive degradation. Previous studies used similar design factors and the mechanistic rationale for maximizing plasma exposure in biomolecules (Pérez-Andrés et al., 2019; Sharafodin and Soltanizadeh, 2022). The conditions of CP treatment are shown in Table 1.

2.6. Techno-functional properties

2.6.1. Water absorption capacity (WAC)

WAC was determined using the method of Langendörfer et al. (2023) and calculated as follows (Equation (1)):

$$\text{WAC (g / hg)} = \frac{W_2 - W_1}{W_0} \times 100 \quad (1)$$

where W_0 is the weight of protein extract (g), W_1 is the weight of the tube plus protein extract and (g), W_2 is the weight of the tube plus the sediment (g) (Langendörfer et al., 2023).

2.6.2. Oil absorption capacity (OAC)

The OAC was determined according to Langendörfer et al. (2023) and calculated using Equation (2):

$$\text{OAC (g / hg)} = \frac{O_2 - O_1}{O_0} \times 100 \quad (2)$$

where O_0 is the weight of sample (g), O_1 is the weight of the tube plus protein extract (g) and O_2 weight of the tube plus the sediment (g) (Langendörfer et al., 2023).

2.6.3. Emulsifying activity (EA) and emulsifying stability (ES)

The EA and ES were determined using Equation (3) (Gani et al., 2022):

$$\text{EA (g / hg)} = \frac{\text{Height of emulsified layer}}{\text{Height of contents of tube}} \times 100 \quad (3)$$

Equation (4) was used to determine ES of the samples:

$$\text{ES (g / hg)} = \frac{\text{Height of remaining emulsified layer}}{\text{Height of original emulsified layer}} \times 100 \quad (4)$$

2.6.4. Foaming capacity (FC) and foaming stability (FS)

FC and FS of the protein extracts were determined using the methods of Lyu et al., 2023. The following Equations (5) and (6) were used to determine FC and FS, respectively.

$$\text{FC (g / hg)} = \frac{\text{Volume after whipping (mL)} - \text{Volume before whipping (mL)}}{\text{Volume before whipping (mL)}} \times 100 \quad (5)$$

$$\text{FS (g / hg)} = \frac{\text{Volume after standing (mL)} - \text{Volume before whipping (mL)}}{\text{Volume before whipping (mL)}} \times 100 \quad (6)$$

2.6.5. Protein solubility (PS)

Solubility of protein extracts was determined according to the method of Ji et al. (2018). Briefly, 1 g/hg solution (10 g/L) of protein extracts in phosphate buffer (0.01 mol/L, pH 7.4) was prepared. This solution was centrifuged at 11,200×*g*, 4 °C for 20 min. The supernatant was collected, and the protein amount was determined according to BCA method. The protein solubility value was calculated using the following Equation (7):

$$\text{Protein solubility (g / hg)} = \frac{\text{Protein content of supernatant } \left(\frac{mg}{mL}\right)}{\text{Total protein content of protein extract } \left(\frac{mg}{mL}\right)} \times 100 \quad (7)$$

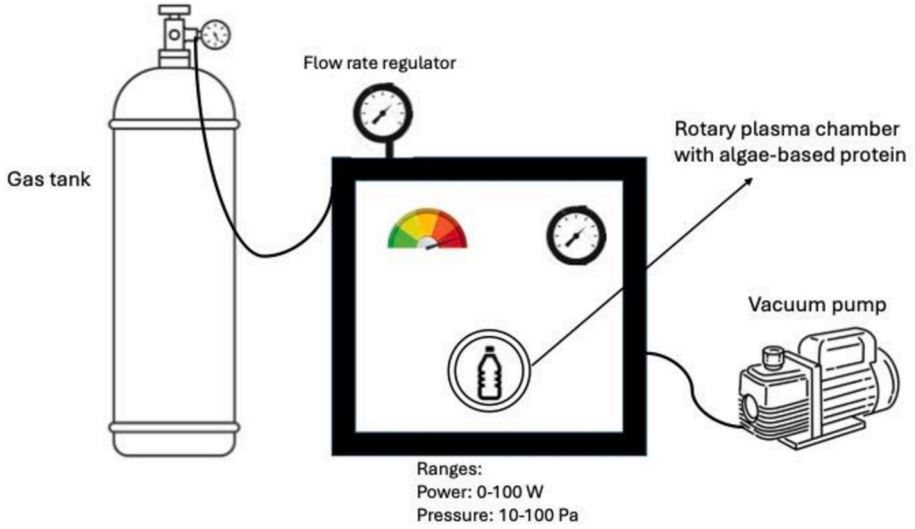


Fig. 2. Schematic diagram of a low-pressure glow discharge cold plasma with rotary chamber (created by using vectorstock.com).

2.6.6. *Free sulfhydryl group analysis (Free-SH)*

Determination of free-SH group content of protein extracts was carried out according to the Ellman method. Equation (8) was used to calculate the amount of free SH (Jiang et al., 2021; Zhang, Huang, Feizollahi, Roopesh, & Chen, 2021):

$$\text{SH (mmol sulfhydryl group / kg protein)} = 73,53 \times (A_{412}) \times D / C \quad (8)$$

A_{412}: Absorbance at 412 nm; C: Sample concentration (g/L) and D: Dilution factor.

2.7. *Antioxidant activity (AOA)*

The cupric reducing antioxidant capacity (CUPRAC) assay was performed using the methodology of Apak, Güçlü, Özyürek, and Karademir (2004). The UV spectrophotometer (Infinite M200, Tecan, Männedorf, Switzerland) was used to measure the absorbance at 450 nm. The 2, 2-diphenyl-1-picrylhydrazyl (DPPH) assay was performed with some modifications and absorbance was measured at 515 nm (Kemal, Teka, Dibaba, & Urugo, M. 2025). The results of CUPRAC and DPPH assays were reported as g of Trolox equivalents (TE) per kg of dw and denoted as AOA_{CUPRAC}, AOA_{DPPH}.

2.8. *Characterization of the protein extracts*

2.8.1. *FT-IR analysis*

Secondary structure of the CP-treated and untreated protein extracts was determined using FT-IR spectroscopy device (Nicolet Summit X FT-IR Spectrometer, Thermo Fisher Scientific, Darmstadt, Germany). All the spectra were average of 18 scans from 4000 cm^{-1} to 400 cm^{-1} at a resolution of 4 cm^{-1}. The raw spectra were processed using OMNIC Paradigm 2.8 HF1 software (Thermos Fisher Scientific, version 2.8.1.31). Background subtraction, baseline correction, Savitzky-Golay filter smoothing, and vector normalization were among the processing steps before peak identification and analysis.

Table 1
Box-Behnken experimental design with extraction conditions and experimentally obtained values of all investigated responses.

Run	Independent variables						Responses									
	A: Power (W)		B: Treatment time (min)		C: Pressure (Pa)		Free SH group (mmol/kg dw)	AOA_{CUPRAC} (g TE/kg dw)	AOA_{DPPH} (g TE/kg dw)	PS (g/hg)	WAC (g/hg)	OAC (g/hg)	EC (g/hg)	ES (g/hg)	FC (g/hg)	FS (g/hg)
1	5.00	−1	15.50	0	90	1	14.24	8.43	10.68	29.49	125.57	255.67	45.41	50.25	55.77	39.41
2	47.50	0	1.00	−1	30	−1	9.98	6.88	0.31	21.39	55.59	261.65	63.18	48.77	35.71	22.43
3	47.50	0	15.50	0	60	0	12.83	7.32	4.04	22.44	108.45	275.40	50.42	52.06	50.91	40.36
4	90.00	1	15.50	0	30	−1	19.76	8.81	7.99	23.01	62.50	284.79	50.45	50.00	47.11	46.00
5	5.00	−1	1.00	−1	60	0	18.84	5.89	0.31	20.70	127.48	341.66	54.17	51.82	51.47	50.08
6	47.50	0	15.50	0	60	0	9.69	6.42	6.59	22.25	40.61	282.80	47.92	49.74	64.94	33.02
7	47.50	0	15.50	0	60	0	19.41	6.39	2.70	18.78	120.75	211.89	54.51	52.48	51.56	52.20
8	47.50	0	15.50	0	60	0	14.70	5.97	4.06	19.89	55.29	264.07	50.00	51.86	57.54	44.87
9	5.00	−1	15.50	0	30	−1	15.38	6.96	0	23.36	178.71	345.18	50.00	54.55	88.56	71.90
10	90.00	1	30.00	1	60	0	21.58	6.96	2.02	20.62	201.42	345.35	50.00	52.48	64.69	40.38
11	90.00	1	1.00	−1	60	0	3.34	9.38	5.29	23.21	271.27	348.85	50.00	53.43	124.01	102.78
12	90.00	1	15.50	0	90	1	25.36	7.50	2.65	22.00	167.66	319.68	50.00	52.06	70.31	45.00
13	47.50	0	1.00	−1	90	1	17.32	7.29	2.99	18.81	297.38	308.71	50.00	47.83	60.02	45.88
14	47.50	0	30.00	1	30	−1	17.06	6.46	2.59	17.82	196.45	311.11	42.81	48.50	53.91	48.23
15	47.50	0	15.50	0	60	0	13.94	6.86	5.19	20.74	110.65	241.35	46.15	49.97	70.91	56.64
16	5.00	−1	30.00	1	60	0	13.03	6.59	0	22.35	163.67	285.78	50.00	50.00	95.97	70.91
17	47.50	0	30.00	1	90	1	9.25	7.35	9.58	25.43	95.61	285.15	50.00	52.06	60.10	42.07

SH: Sulfhydryl, AOA_{CUPRAC}: Antioxidant activity by cupric reducing antioxidant capacity; AOA_{DPPH}: Antioxidant activity by 2,2-diphenyl-1-picrylhydrazyl radical scavenging, PS: Protein solubility, WAC: Water absorption capacity, OAC: Oil absorption capacity, EC: Emulsion capacity, ES: Emulsion stability, FC: Foaming capacity, FS: Foaming stability.

2.8.2. SEM analysis

Morphological characterization was conducted to understand the changes in surface morphology using SEM (JSM-6700 F, JEOL, Tokyo, Japan). The operation was performed at an acceleration voltage of 2 kV, and micrographs of the samples were captured at 1000× and 2500 × magnifications. Before using SEM, the freeze-dried protein extracts were sprayed with gold (Escobar Cano et al., 2024; Zhang et al., 2022).

2.9. Color attributes

Color changes in the modified and unmodified protein extracts were determined using the spectrophotometer (CM-5, Konica Minolta, Langenhagen, Germany). The results were determined as changes in redness/greenness, yellowness/blueness and brightness/darkness (a*, b*, and L*). The total color difference (ΔE), chroma index (C), hue angle (H), whiteness index (WI), and browning index (BI) were determined using Equations (9)–(13) (Akgün et al., 2020).

$$\Delta E = \sqrt{\Delta L^{*2} + \Delta a^{*2} + \Delta b^{*2}} \tag{9}$$

$$SI = \sqrt{a^{*2} + b^{*2}} \tag{10}$$

$$C = \tan^{-1} \times \frac{b}{a} \tag{11}$$

$$WI = 100 - \sqrt{(100 - L^{*})^2 + a^{*2} + b^{*2}} \tag{12}$$

$$BI = \frac{(x - 0.31)}{0.17} \times 100 \tag{13}$$

2.10. Nutritional properties of the protein extracts

2.10.1. Amino acid composition

Chemical hydrolysis of the protein extracts was carried out using 6 mol/L HCl. Firstly, the protein extracts having 100 mg protein content and 10 mL of HCl were mixed and sealed hermetically. This solution was kept in the sand bath for 16 h at 100 °C. After cooling the samples to room temperature, sodium hydroxide solution (6 mol/L) was added to neutralize. The samples were then filtered in a volumetric flask with a folded filter and filled to 50 mL with ultra-pure water. Then, 2 mL of the samples were centrifuged at 30,000×*g* for 5 min and the supernatant was transferred into a 2 mL reaction tube (Dai et al., 2014).

The HPLC-FLD analysis of total and free amino acids was performed after derivatization using ortho-phthalaldehyde (OPA). HPLC equipment (Smartline 1000, Knauer Gerätebau GmbH, Berlin, Germany) was equipped with a fluorescence detector (RF-20A, Shimadzu, Kyoto, Japan), auto-sampler AS 6.1 L, pump 6.1 L, gradient former, and degasser. Separations were carried out on a reversed phase column (Gemini 5 μm C18, 150 × 4.6 mm, Phenomenex, Aschaffenburg, Germany).

2.10.2. Nutritional properties

The nutritional value of the modified and unmodified protein extracts was explained using Equation (14). Amino acid score (AAS) (%) was calculated using Equation (14) and used the reports of Food and Agriculture Organization (FAO)/World Health Organization (WHO) (FAO/WHO, 2007):

$$AAS\ (g/hg) = \frac{\text{mg of amino acid per g protein sample}}{\text{mg of amino acid per g of FAO and WHO standard pattern}} \times 100. \tag{14}$$

Essential amino acid (EAA) score was calculated using Equation (15) according to the method of FAO (Huang et al., 2019):

$$EAA(g/hg) = \frac{\text{mg of EAA in per g protein sample}}{\text{mg of EAA in per g of egg protein}} \times 100 \tag{15}$$

According to Onyenweaku et al. (2022), essential amino acid content of egg is 27.16 g/hg.

2.11. Experimental design and statistical analysis

The Box-Behnken Design (BBD)-based Response Surface Methodology was employed to optimize CP conditions. Power (5, 47.50, and 90 W), pressure (30, 60, and 90 Pa), and treatment time of 1, 15, and 30 min were the independent variables (Table 1). There are 17 experimental runs in the design with five replicates at central points and twelve factorial points. The regression coefficients (β) were obtained by fitting the response variables to a second-order polynomial model. Equation (16) was utilized in the response surface analysis of the generalized second-order polynomial model:

$$Y = \beta_0 + \beta_1 X_1 + \beta_2 X_2 + \beta_3 X_3 + \beta_{11} {X_1}^2 + \beta_{22} {X_2}^2 + \beta_{33} {X_3}^2 + \beta_{12} X_1 X_2 + \beta_{13} X_1 X_3 + \beta_{23} X_2 X_3 + \epsilon\pi r^2 \tag{16}$$

The regression coefficient is defined as β_0 for constant, β_i for linear, β_{ii} for quadratic and β_{ij} for interaction effect term. Regression coefficients, statistical significance, and model appropriateness were assessed using the analysis of variance (ANOVA).

Design Expert 7.1 software (Stat-Ease, Inc., MN, USA) was used to conduct the statistical analysis. A significance level of $p = 0.05$ was used for statistical analysis of the data. Appropriateness of the model was evaluated using the coefficient of determination (R^2) and model weakness. The impact of a single process parameter and/or the interaction of multiple parameters on each response under investigation was described by a mathematical model.

Minitab (Version 17, Minitab Inc., State College, PA) was used for statistical analysis of color and amino acid profile analysis. The Tukey test was used to compare the variations in mean values. The differences between mean values were compared using the Tukey test (differences at $p \leq 0.05$ were significant). The optimization studies and all analysis were carried out in triplicate and data were given as mean ± standard deviation.

3. Results and discussion

3.1. Goodness of fitting

Free SH group, AOA_{CUPRAC}, AOA_{DPPH}, WAC, OAC, EC, ES, FC, FS, and PS were determined as functions of linear, quadratic and interaction in terms of the independent variables including power, treatment time and pressure using BBD (Table 1). Analysis of variance and coefficients of the model (R^2) for each dependent variable are indicated in Table 2. The R^2 values were 0.6926, 0.8278, 0.7871, 0.8256, 0.8317, 0.7848, 0.7256, 0.6139, 0.8287, and 0.7324 for free SH group, AOA_{CUPRAC}, AOA_{DPPH}, PS, WAC, OAC, EC, ES, FC, and FS, respectively (Table 2). The lack of fit test showed no significant lack of fit ($p > 0.05$) and thus the model suitably fits with the data. The lack of fit of SH group, AOA_{CUPRAC}, AOA_{DPPH}, PS, WAC, OAC, EC, ES, FC, and FS was not significant, and their p values were 0.2109, 0.2734, 0.0939, 0.3335, 0.2169, 0.5330,

Table 2
Analysis of variance (ANOVA) of the fitted second-order polynomial model obtained in this study.

Source	Sum of squares	DF	Mean square	F-value	p-value
Free sulfhydryl groups (mmol sulphydril group/kg protein dw)					
Model	311.67	9	34.63	1.75	0.2360
Linear					
$ß_1$	3.97	1	3.97	0.20	0.6676
$ß_2$	35.42	1	35.42	1.79	0.2225
$ß_3$	0.41	1	0.41	0.021	0.8900
Interaction					
$ß_{12}$	144.59	1	144.59	7.32	0.0304*
$ß_{13}$	11.35	1	11.35	0.57	0.4732
$ß_{23}$	57.30	1	57.30	2.90	0.1324
Quadratic					
$ß_{11}$	30.24	1	30.24	1.53	0.2560
$ß_{22}$	28.44	1	28.44	1.44	0.2693
$ß_{33}$	15.03	1	15.03	0.76	0.4120
Residual	138.35	7	19.76	–	–
Lack of fit	88.63	3	29.54	2.38	0.2109
Pure error	49.72	4	12.43	–	–
Cor total	450.02	16	–	–	–
$R^2 = 0.6926$; C.V.(%) = 29.56					
Antioxidant activity by CUPRAC (g TE/kg dw)					
Model	12.17	9	1.35	3.74	0.0479*
Linear					
$ß_1$	4.02	1	4.02	11.13	0.0125*
$ß_2$	0.60	1	0.60	1.67	0.2376
$ß_3$	0.010	1	0.010	0.029	0.8696
Interaction					
$ß_{12}$	2.43	1	2.43	6.73	0.0357*
$ß_{13}$	1.93	1	1.93	5.33	0.0543
$ß_{23}$	0.058	1	0.058	0.16	0.7013
Quadratic					
$ß_{11}$	2.52	1	2.52	6.96	0.0335*
$ß_{22}$	0.11	1	0.11	0.29	0.6044
$ß_{33}$	1.33	1	1.33	3.67	0.0971
Residual	2.53	7	0.36	–	–
Lack of fit	1.48	3	0.49	1.88	0.2734
Pure error	1.05	4	0.26	–	–
Cor total	14.70	16	–	–	–
$R^2 = 0.8278$; C.V.(%) = 8.42					
Antioxidant activity by DPPH (g TE/kg dw)					
Model	134.76	9	14.97	2.87	0.0889
Linear					
$ß_1$	20.66	1	20.66	3.97	0.0867
$ß_2$	1.49	1	1.49	0.29	0.6092
$ß_3$	10.70	1	10.70	2.05	0.1949
Interaction					
$ß_{12}$	2.20	1	2.20	0.42	0.5365
$ß_{13}$	64.17	1	64.17	12.32	0.0099*
$ß_{23}$	4.63	1	4.63	0.89	0.3771
Quadratic					
$ß_{11}$	1.40	1	1.40	0.27	0.6203
$ß_{22}$	17.49	1	17.49	3.36	0.1095
$ß_{33}$	8.13	1	8.13	1.56	0.2516
Residual	36.46	7	5.21	–	–
Lack of fit	27.94	3	9.31	4.38	0.0939
Pure error	8.51	4	2.13	–	–
Cor total	171.22	16	–	–	–
$R^2 = 0.7871$; C.V.(%) = 57.93					

Source	Sum of squares	DF	Mean square	F-value	p-value
Protein solubility (g/hg)					
Model	99.38	9	11.04	3.68	0.0499*
Linear					
$ß_1$	2.04	1	2.04	0.68	0.4371
$ß_2$	0.45	1	0.45	0.15	0.7111
$ß_3$	3.09	1	3.09	1.03	0.3441
Interaction					
$ß_{12}$	4.49	1	4.49	1.50	0.2605
$ß_{13}$	12.72	1	12.72	4.24	0.0785
$ß_{23}$	25.97	1	25.97	8.66	0.0216*
Quadratic					
$ß_{11}$	21.34	1	21.34	7.11	0.0321*
$ß_{22}$	7.68	1	7.68	2.56	0.1535
$ß_{33}$	8.19	1	8.19	2.73	0.1425
Residual	21.00	7	3.00	–	–

(*continued on next page*)

Table 2 (*continued*)

Source	Sum of squares	DF	Mean square	F-value	p-value
Lack of fit	11.27	3	3.76	1.55	0.3335
Pure error	9.73	4	2.43	–	–
Cor total	120.38	16	–	–	–
$R^2 = 0.8256$; C.V.(%) = 7.91					
Water absorption capacity (g/hg)					
Model	71965.62	9	7996.18	3.84	0.0449*
Linear					
$ß_1$	225.21	1	225.21	0.11	0.7518
$ß_2$	208.93	1	208.93	0.10	0.7606
$ß_3$	2646.67	1	2646.67	1.27	0.2966
Interaction					
$ß_{12}$	2811.67	1	2811.67	1.35	0.2832
$ß_{13}$	6264.74	1	6264.74	3.01	0.1263
$ß_{23}$	29349.93	1	29349.93	14.10	0.0071*
Quadratic					
$ß_{11}$	6106.20	1	6106.20	2.93	0.1304
$ß_{22}$	18190.52	1	18190.52	8.74	0.0212*
$ß_{33}$	295.49	1	295.49	0.14	0.7175
Residual	14567.09	7	2081.01	–	–
Lack of fit	9251.27	3	3083.76	2.32	0.2169
Pure error	5315.82	4	1328.96	–	–
Cor total	86532.71	16	–	–	–
$R^2 = 0.8317$; C.V.(%) = 32.60					
Oil absorption capacity (g/hg)					
Model	19843.68	9	2204.85	2.84	0.0915
Linear					
$ß_1$	49.20	1	49.20	0.063	0.8086
$ß_2$	2.11	1	2.11	2.715E-003	0.9599
$ß_3$	198.21	1	198.21	0.26	0.6290
Interaction					
$ß_{12}$	686.23	1	686.23	0.88	0.3787
$ß_{13}$	3869.05	1	3869.05	4.98	0.0609
$ß_{23}$	1333.23	1	1333.23	1.72	0.2316
Quadratic					
$ß_{11}$	7602.40	1	7602.40	9.78	0.0167*
$ß_{22}$	4533.97	1	4533.97	5.83	0.0464*
$ß_{33}$	58.80	1	58.80	0.076	0.7912
Residual	5439.77	7	777.11	–	–
Lack of fit	2123.89	3	707.96	0.85	0.5330
Pure error	3315.88	4	828.97	–	–
Cor total	25283.45	16	–	–	–
$R^2 = 0.7848$; C.V.(%) = 9.54					

Source	Sum of squares	DF	Mean square	F-value	p-value
Emulsion capacity (g/hg)					
Model	219.30	9	24.37	2.06	0.1771
Linear					
$ß_1$	0.071	1	0.071	6.000E-003	0.9404
$ß_2$	123.71	1	123.71	10.44	0.0144*
$ß_3$	10.41	1	10.41	0.88	0.3798
Interaction					
$ß_{12}$	4.34	1	4.34	0.37	0.5641
$ß_{13}$	4.28	1	4.28	0.36	0.5669
$ß_{23}$	103.80	1	103.80	8.76	0.0211*
Quadratic					
$ß_{11}$	1.75	1	1.75	0.15	0.7124
$ß_{22}$	14.99	1	14.99	1.27	0.2978
$ß_{33}$	0.15	1	0.15	0.013	0.9135
Residual	82.94	7	11.85	–	–
Lack of fit	43.55	3	14.52	1.47	0.3486
Pure error	39.40	4	9.85	–	–
Cor total	302.25	16	–	–	–
$R^2 = 0.7256$; C.V.(%) = 6.84					
Emulsion stability (g/hg)					
Model	33.26	9	3.70	1.24	0.3985
Linear					
$ß_1$	0.16	1	0.16	0.054	0.8226
$ß_2$	0.041	1	0.041	0.014	0.9096
$ß_3$	1.41	1	1.41	0.47	0.5147
Interaction					
$ß_{12}$	0.19	1	0.19	0.064	0.8075
$ß_{13}$	10.12	1	10.12	3.39	0.1083
$ß_{23}$	5.08	1	5.08	1.70	0.2336
Quadratic					
$ß_{11}$	10.36	1	10.36	3.47	0.1049

(*continued on next page*)

Table 2 (*continued*)

Source	Sum of squares	DF	Mean square	F-value	p-value
$ß_{22}$	3.09	1	3.09	1.04	0.3428
$ß_{33}$	4.87	1	4.87	1.63	0.2425
Residual	20.92	7	2.99	–	–
Lack of fit	14.43	3	4.81	2.96	0.1606
Pure error	6.49	4	1.62	–	–
Cor total	54.18	16	–	–	–
$R^2 = 0.6139$ C.V.(%) = 3.39					
Foaming capacity (g/hg)					
Model	5894.76	9	654.97	3.76	0.0473*
Linear					
$ß_1$	7.50	1	7.50	0.043	0.8415
$ß_2$	13.28	1	13.28	0.076	0.7904
$ß_3$	361.85	1	361.85	2.08	0.1926
Interaction					
$ß_{12}$	2695.26	1	2695.26	15.48	0.0056*
$ß_{13}$	783.75	1	783.75	4.50	0.0716
$ß_{23}$	82.08	1	82.08	0.47	0.5144
Quadratic					
$ß_{11}$	1509.81	1	1509.81	8.67	0.0216*
$ß_{22}$	148.03	1	148.03	0.85	0.3872
$ß_{33}$	675.66	1	675.66	3.88	0.0895
Residual	1218.90	7	174.13	–	–
Lack of fit	918.83	3	306.28	4.08	0.1038
Pure error	300.06	4	75.02	–	–
Cor total	7113.66	16	–	–	–
$R^2 = 0.8287$; C.V.(%) = 20.33					

Source	Sum of squares	DF	Mean square	F-value	p-value
Foaming stability (g/hg)					
Model	3843.13	9	427.01	2.13	0.1658
Linear					
$ß_1$	13.34	1	13.34	0.067	0.8039
$ß_2$	6.93	1	6.93	0.035	0.8578
$ß_3$	30.24	1	30.24	0.15	0.7093
Interaction					
$ß_{12}$	1731.95	1	1731.95	8.63	0.0218*
$ß_{13}$	247.90	1	247.90	1.24	0.3030
$ß_{23}$	219.26	1	219.26	1.09	0.3305
Quadratic					
$ß_{11}$	1047.16	1	1047.16	5.22	0.0562
$ß_{22}$	98.94	1	98.94	0.49	0.5052
$ß_{33}$	474.21	1	474.21	2.36	0.1680
Residual	1404.12	7	200.59	–	–
Lack of fit	1052.70	3	350.90	3.99	0.1071
Pure error	351.41	4	87.85	–	–
Cor total	5247.25	16	–	–	–
$R^2 = 0.7324$; C.V.(%) = 28.25					

*Significant at $p \leq 0.05$, β_1: Power (watt), β_2: Treatment time (min), β_3: Pressure (Pa).

0.3486, 0.1606, and 0.1038, respectively (Table 2). These results demonstrate that the model for AOA_{CUPRAC}, PS, WAC, and FC can be used to optimize the modification conditions of proteins from *C. prolifera* with cold plasma. Equations (17)–(20) that predict the relationship between the independent and response variables in terms of coded factors:

$$AOA_{CUPRAC} = 6.58 + 0.74 \times A - 0.29 \times B - 0.050 \times C\text{-}0.78 \times AB - 0.83 \times AC + 0.14 \times BC + 0.77 \times A^2 - 0.16 \times B^2 + 0.81 \times C^2 \quad (17)$$

$$PS = 20.62\text{–}0.52 \times A - 0.25 \times B + 0.85 \times C - 1.06 \times AB - 2.14 \times AC + 3.06 \times BC + 2.25 \times A^2 - 1.35 \times B^2 + 2.01 \times C^2 \quad (18)$$

$$WAC = 82.66 + 5.51 \times A + 5.31 \times B + 24.92 \times C - 26.51 \times AB + 47.49 \times AC - 102.79 \times BC + 38.08 \times A^2 + 65.73 \times B^2 + 12.06 \times C^2 \quad (19)$$

$$FC = 58.14\text{–}1.01 \times A + 1.34 \times B + 9.22 \times C - 25.96 \times AB + 16.80 \times AC - 5.44 \times BC + 18.94 \times A^2 + 5.93 \times B^2 - 18.24 \times C^2 \quad (20)$$

A: Power (W), B: Treatment time (min), C: Pressure (Pa). AOA_{CUPRAC}: Antioxidant activity by cupric reducing antioxidant capacity; PS: Protein solubility; WAC: Water absorption capacity; FC: Foaming capacity.

3.2. Protein extraction

In our previous study, protein content of protein extract from *C. prolifera* was found as 51.57 g/kg under extraction temperature of 30 °C, extraction time of 60.03 min and enzyme/substrate ratio of 0.20 (*w/w*) (Yucetepe et al., 2022). In the present study, PC of protein extract from *C. prolifera* was 608.96 ± 12.73 g/kg in dw. Carbohydrase enzymes are used to break down cell walls and make extraction of bioactive compounds easier (Liu, Gasmalla, & Yang, 2016). Therefore, a substrate/hemicellulose enzyme ratio of 1:1 (*w/w*) was applied in the present study, and a higher protein content (608.96 ± 12.73 g/kg dw) was obtained compared to that of our previous study (Yucetepe et al., 2022). A higher concentration of enzyme would typically increase solubility of the protein in the extraction and, thus, the extraction yield (Shen et al., 2008). Macroalgae cell walls are more chemically complicated than those of terrestrial plants since they mostly consist of cellulose and hemicellulose. The ability of enzymes to hydrolyze components of macroalgae cell wall, disrupting its structural complexity by creating an enzyme-substrate complex and releasing the cell contents into the solution, is often the primary basis for enzyme-assisted extraction for macroalgae (Sanjeewa et al., 2023).

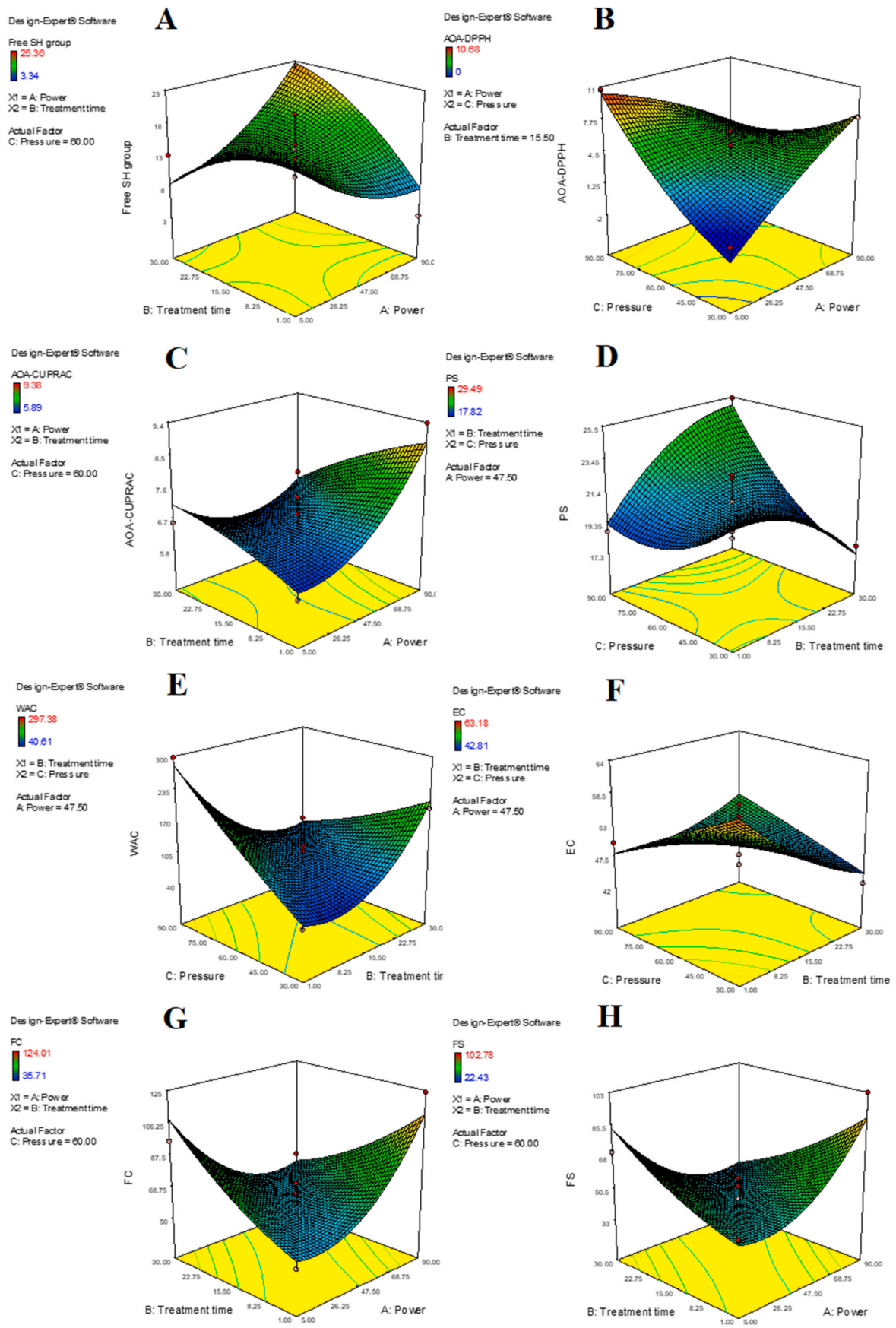


Fig. 3. A-H. 3D contour plot response surface for the effect of cross-interaction between power treatment time and pressure on various properties of CP-treated protein extracts, including free sulfhydryl group content (Free-SH group) (A), antioxidant activity (AOA) by DPPH method (B), antioxidant activity by CUPRAC method (C), water absorption capacity (WAC) (D), protein solubility (PS) (E), emulsion capacity (EC) (F), foaming capacity (FC) (G), foaming stability (FS) (H).

3.3. Optimization studies

3.3.1. Free sulfhydryl groups content

Free sulfhydryl group content of the extracts changed from 3.34 to 25.36 mmol/kg dw (Table 1). Free SH content of the control sample (i.e., untreated/unmodified protein extracts) was 7.98 mmol/kg dw. According to Fig. 3A, an increase in power and treatment time is associated with a notable increase in free SH group concentrations, suggesting that higher treatment times promote conformational changes and increased thiol group accessibility. Thiol groups in two cysteine molecules next to or in the same polypeptide chain may interact to produce inter/intramolecular disulfide connections when protein molecular structure is oxidized during CP treatment because of the entry of numerous chemicals with high oxidation potential, such as OH−, H_2O_2, O_3 (H_2O_2 + R-SH → R-S-S-R + $2H_2O$) (Yu et al., 2023). The oxidation of sulfur-containing amino acid residues may break down sulfhydryl groups during CP application. The disulfide bonds were converted into free sulfhydryl groups with the prolongation of time. This is cause of proteins oxidize because of reactive species formed during CP treatment (X. Y. Wang et al., 2024; P. Wang et al., 2024). Similarly, the study of Zhang et al. (2021), free SH group content of pea proteins increased after cold plasma application. Free SH groups increased due to the unfolding of proteins and thus, water absorption capacity and emulsion capacity of walnut protein increased. The increase in SH group is attributed to the breaking of disulfide bonds following the hydration of disulfide (S-S) bonds in proteins (Zhang et al., 2021). Lambrecht et al. (2018) reported that S-S bond in glutenin protein can react with water to form SH group, thereby causing an increase in SH group level in flour protein. In contrast, cross-linking of SH groups to form intermolecular S-S bonds between protein subunits results in a decrease in SH groups (Kumar et al., 2021).

3.3.2. Antioxidant activity

The AOA of the extracts ranged from 5.89 to 9.38 g TE/kg dw with CUPRAC method and from 0 to 10.68 g TE/kg dw with DPPH method (Table 1), respectively. AOA of the control sample was found as 4.41 ± 0.05 g TE/kg dw and 2.53 ± 0.41 g TE/kg dw with CUPRAC and DPPH methods, respectively. At CP conditions of ~30 W power and 80 Pa pressure, the highest AOA_{DPPH} values were obtained according to Fig. 3B. AOA $_{CUPRAC}$ consistently increased at power >80 W and treatment time of 1-to ~8 min (Fig. 3C). This trend showed that the highest power levels stimulated release of antioxidant compounds and enhanced antioxidant activity, highlighting the critical role that the interaction between treatment time and power played in controlling antioxidant activity of the protein extracts (Fig. 3C). AOA $_{CUPRAC}$ values of the protein extracts were determined by linear and quadratic effects of power as well as the interaction effect between power and treatment time. These findings suggested that AOA was significantly shaped by level and duration of applied energy ($p < 0.05$, Table 2). The results obtained are consistent with previous data from the literature (Kashfi et al., 2020; X. Li et al., 2019; X. Y. Wang et al., 2024). This phenomenon may have occurred because of the higher energy density which caused reactive species, charged particles, and UV photons to break down cell membrane and covalent bonds of the sample, releasing antioxidant compounds during CP application (Wang et al., 2025). Moreover, thiol molecules with a carbon-bonded sulfhydryl group are involved in redox signaling, biological process regulation, and cellular antioxidant defenses by controlling the composition of disulfide links in proteins. Many researchers have conducted in-depth studies on -SH as antioxidants and metal antidotes to date (Charlton et al., 2023; Han et al., 2024; Roshanfekr et al., 2025). For instance, Yu et al. (2021) showed that an increase in free radical scavenging capacity was observed with increasing in SH groups after CP application to peanut proteins. Therefore, it can be stated that a decrease in S-S bonds between the molecules can result in an increase in SH groups, as mentioned in Section 3.3.1, resulting in an increase in AOA after CP application.

3.3.3. Protein solubility

PS of CP-treated protein extracts changed between 17.82 and 29.49 g/hg while PS of control sample was 16.42 ± 0.69 g/hg (Table 1). Table 2 shows that PS of CP-treated protein extracts was significantly affected by the quadratic effect of power and the interaction effect between treatment time and pressure ($p < 0.05$, Table 2). The sensitivity of protein structural characteristics to combined processing parameters given in Table 1 independent variables with their different levels was shown by a clear increasing trend in PS values, which increased as treatment time increased from 8 to 30 min and pressure increased from 70 to 90 Pa (Fig. 3D). Similarly, Zhang et al. (2020) reported that the protein solubility of soy protein isolates increased after CP application. The reactive species generated during plasma application can enhance the binding and interaction of water molecules with the protein surface through hydrophilic groups (Zhang et al., 2020). In addition, the increase in PS with increasing voltage and application time was associated with the surface charges and particle sizes of proteins (Bußler et al., 2015). Wang et al. (2024) reported that proteins exhibited an increasing tendency as treatment duration increased. The exposure of the active sites and the increase in surface roughness could be the result of the energetic particles that attacked the proteins. Solubility may be increased by some basic amino acid side chains reacting with the reactive ions produced by CP. Moreover, hydrophilic groups of proteins are exposed when they are treated with plasma, increasing their solubility (X. Y. Wang et al., 2024). On the other hand, in the study of Kumar et al. (2021), cross-linking of free-SH groups to form S-S bonds between protein subunits resulted in aggregation of proteins in flour, which was also supported by the decrease in solubility of proteins.

3.3.4. Water and oil absorption capacity

WAC and OAC are among the key techno-functional properties of proteins since they greatly influence the texture of foods like minced meat, mayonnaise, baked dough, and dairy products (Rout and Srivastav, 2024). In this study, WAC and OAC of the modified protein extracts ranged between 40.61 and 297.38 g/hg and 211.89 and 348.85 g/hg, respectively (Table 1). WAC and OAC of the untreated protein extracts were 93.11 ± 30.08 g/hg and 332.46 ± 29.54 g/hg, respectively. The interaction between treatment time and pressure and the quadratic effect of treatment time were significant on WAC of the samples ($p < 0.05$, Table 2). Moreover, the quadratic effect of power and treatment time had a significant effect on OAC of the protein extracts after CP application ($p < 0.05$, Table 2). The combination of high pressure and low treatment time produced the highest WAC values (Fig. 3E). Additionally, treating for 20–30 min at pressure between 40 and 70 Pa caused noticeable improvements in WAC (Fig. 3E), indicating that a balanced approach to processing time and pressure is essential for maximizing water absorption capacity of the protein extracts. Cell walls may be damaged because of protein structural changes by CP application at both higher and lower power levels. Furthermore, WAC of proteins is influenced by the hydrophobic and hydrophilic balance of amino acids as well as the protein structure (Chen et al., 2019). For instance, according to Basak and Annapure, 2022, the decrease in surface hydrophobicity and the increase in surface water distribution are the factors that contribute to the high-water absorption capacity. CP application resulted in a high-water absorption capacity and a decrease in surface hydrophobicity due to the increased surface area and hydrophilic groups of peanut protein isolates (Ji et al., 2019). The findings of WAC analysis suggest that proteins from *C. prolifera*, modified by CP, might be good candidates for improving the WAC of foods as desirable WAC values range between 149 and 472 g/hg in food applications (Chen et al., 2019).

3.3.5. Emulsifying and foaming properties

Proteins have a remarkably high potential to form emulsions due to their interaction with lipids, which is commonly observed in many food systems (Rout and Srivastav, 2024). In this study, EC and ES of the

modified protein extracts ranged from 42.81 to 63.18 g/hg and from 47.83 to 54.55 g/hg, respectively (Table 1). The linear effect of treatment time and interaction effect of treatment time and pressure were significant on EC of the protein extracts after CP treatment ($p < 0.05$, Table 2). The explanation for this behavior can also be derived from solubility results as mentioned in Section 3.3.3. Higher solubility proteins can more easily reach water-oil contact during emulsification. According to Fig. 3F, the highest EC values were obtained at treatment time of 1–4 min and pressure of 40–50 Pa. Similarly, in another study, emulsion stability of peanut protein isolate emulsions increased progressively during the 2-min CP treatment and peaked at 2 min (Ji et al., 2018).

FC and FS of the modified proteins ranged from 35.71 to 124.01 g/hg and from 22.43 to 102.78 g/hg, respectively (Table 1). EC and ES of control sample were 46.86 ± 2.63 g/hg and 46.31 ± 1.85 g/hg, and FC and FS were 49.20 ± 0.17 g/hg and 28.69 ± 5.70 g/hg, respectively. The interaction effect of power and treatment time for FC and FS and quadratic effect of power were significant for FC ($p < 0.05$, Table 2). These findings suggest that interactions between power and treatment time, rather than their individual contributions, determine the foaming properties of the protein extracts. Foams with higher stability were produced by both the lowest and the highest levels of treatment time and power than those under moderate conditions (Fig. 3G and H). Low-frequency short-term plasma application can lead to more flexible structures with the capacity to form films at the oil-water or air-water interface, which has positive aspects in terms of emulsification and foaming properties. Extensive conformational changes and the breaking of disulfide bonds at high levels of treatment time and power may result in more reactive groups that significantly enhance foam structure, whereas limited structural unfolding at moderate levels of treatment time and power may reveal surface-active sites that maximize foam stability. In the present study, it was observed that FC of the protein extracts increased after CP treatment. Similarly, Zhang et al. (2020) showed that CP systems with low frequency (80 Hz) of soy protein achieved better emulsification and foaming properties than those with higher frequency (120 Hz).

3.4. Optimization and verification

The optimum conditions of CP treatment were as follows: power of 87.50 W, treatment time of 6.63 min and pressure of 90 Pa. Predicted and mean experimental values for WAC (267.72 and 232.04 ± 10.25 g/hg), OAC (345.40 and 350.66 ± 15.78 g/hg), EC (47.83 and 49.50 ± 5.05 g/hg), ES (50.83 and 49.95 ± 0.51 g/hg), FC (96.20 and 101.26 ± 7.89 g/hg), FS (69.08 and 70.10 ± 2.85 g/hg), Free-SH group content (20.16 and 18.28 ± 1.50 mmol/kg dw), AOA_{DPPH} (3.39 and 3.78 ± 0.40 g/kg dw), AOA_{CUPRAC} (8.34 and 8.31 ± 0.01 g/kg dw), and PS (22.20 and 22.30 ± 4.02 g/hg) indicated that the differences between the predicted and mean experimental values were not significant ($p \geq 0.05$). Moreover, characterization studies and color and nutritional properties of the modified protein extracts prepared under the optimized CP conditions were investigated.

3.5. Characterization studies

3.5.1. FT-IR

The FT-IR spectrum of the untreated and CP-treated protein extracts contained several typical bands for functional groups with variances in the absorption strength of some distinctive peaks. The typical group frequencies of proteins in secondary structures are amide I (1700-1600 cm^{-1}), amide II (1600-1500 cm^{-1}), and amide III (1200–1300 cm^{-1}) (Fig. 4). Amide I is a representation of protein aggregation, folding, and unfolding the results from C-O stretching vibration of the carbonyl group. Amide II and III, which are more intricate and conformationally sensitive, typically result from H-N-C bending and CO-NH stretching. Changes in secondary protein structural composition are identified using the amide region (Monica et al., 2025). The broad band approximately 3250 cm^{-1} (amide A) can be attributed to stretching vibrations of the O−H and N−H groups (Abdul-Enein, Bunaciu, & Fleschin, 2014). In the FT-IR spectrum, amide I is shown at ~1585 cm^{-1} (extending as C=O free carboxyl groups). Amide II band (~1392 cm^{-1}) is due to the presence of stretching of C−N and bending vibrations of N−H groups (Andrade et al., 2019; Kong & Yu, 2007). The peaks at about 1268 cm^{-1} represent the amide III bands (C–C, C–N and C–O stretching). The bands prove the presence of proteins in the analyzed extract (Withana-Gamage, Wanasundara, Pietrasik, & Shand, 2011). In addition, the peaks at 1000-1100 cm^{-1} are attributed to the C−O−C band, showing the existence of polysaccharides in macroalgal cell walls (Gómez-Ordóñez & Rupérez, 2011). According to Fig. 4, the untreated and peak positions of CP-treated proteins are almost identical, but there are variations in their intensities ($p < 0.05$). Especially, the decrease in band intensities of amide I, II, III, A and B ($p < 0.05$) following CP treatment indicated that reactive species of the plasma caused structural change, partial denaturation, or oxidation of proteins. The variations in

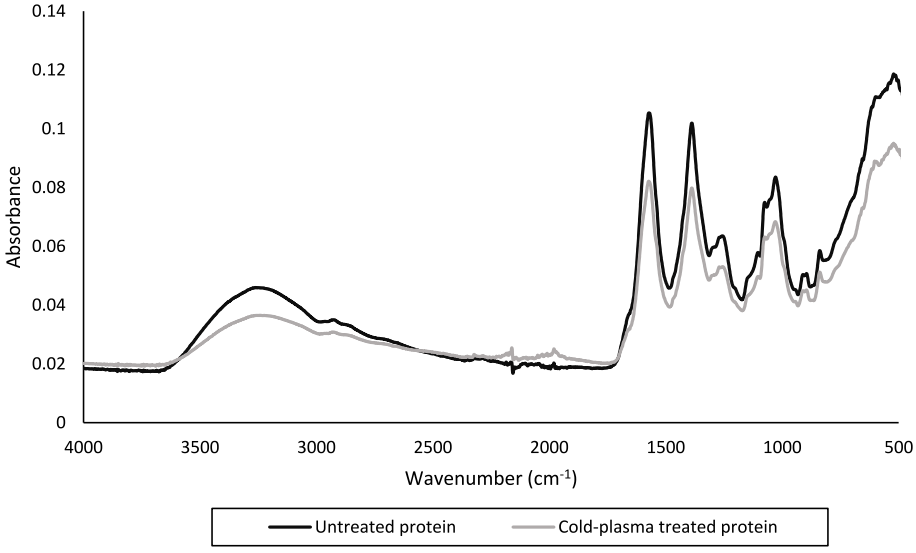


Fig. 4. FT-IR spectra of control (black) and cold plasma-treated (power of 87.50 W, treatment time of 6.63 min and pressure of 90 Pa) protein extracts from *Caulerpa prolifera* (grey).

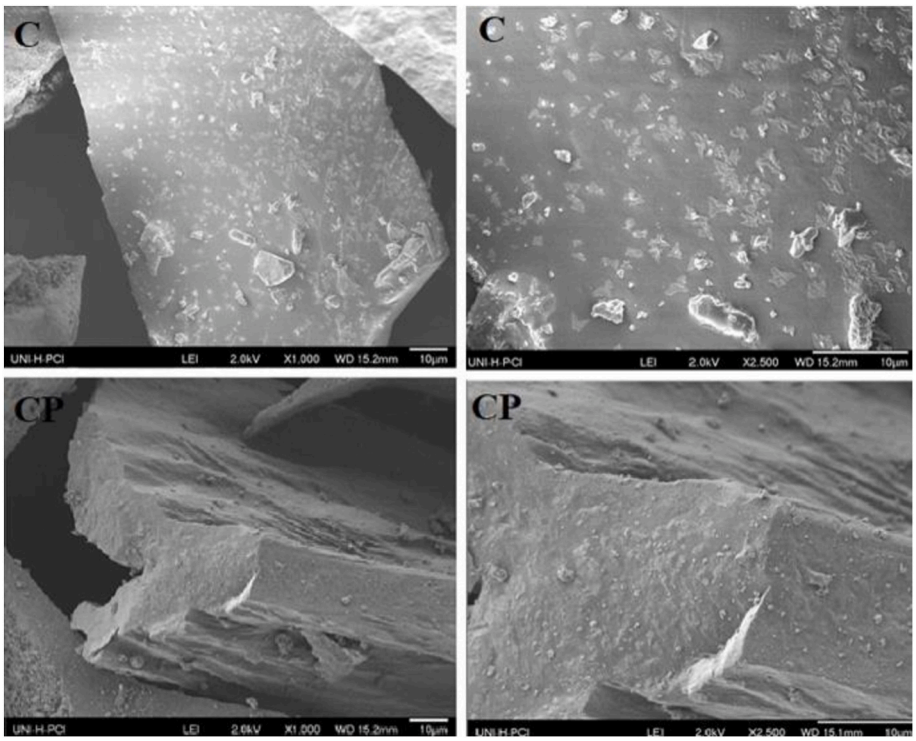


Fig. 5. SEM images of control and cold plasma-treated (power of 87.50 W, treatment time of 6.63 min and pressure of 90 Pa) protein extracts from *Caulerpa prolifera*. The images on the left were magnified 1,000 times and the images on the right were magnified 2,500 times with 10 micrometer scale all of them.

the amide I band indicate changes in the secondary structure of proteins (Sharma & Singh, 2020).

FT-IR provides information on protein secondary structure changes by analyzing changes in chemical bonding within amide I bond (1600–1700 cm^{-1}). The secondary structure of the protein backbone is made up of the α-helix, β-sheet, β-turn, and aperiodic structures. A previous study (De Meutter & Goormaghtigh, 2021) has demonstrated that side-chain contributions in the amide I–II region may inhibit secondary structure estimation; therefore, a decrease in intensity of these bands could indicate side-chain oxidation or cleavage as well as changes in the α-helix/β-sheet content and the resulting hydrogen-bond network (B. Li, Peng, et al., 2024; M. Li, Peng, et al., 2024; X. Li et al., 2019).

In addition to decreased intensities of amide I–III and amide A–B bands, CP caused in an increase in 3_{10}-helix content and β-turn and a decrease in β-sheet structure. The percentages of 3_{10}-helix and β-turn structures increased from 18.6 % to 20.1 % and 15.5 %–20.1 % for the untreated and CP-treated proteins, respectively ($p < 0.05$). Conversely, the β-sheet composition of the untreated and CP-treated proteins decreased from 65.8 % to 59.7 %, respectively ($p < 0.05$). Similarly, peanut protein isolate displayed a decrease in β-sheet content and an increase in β-turn content following 3 min of CP treatment (B. Li, Peng, et al., 2024). These changes suggest that the protein backbone has partially unfolded and rearranged, with some β-sheet segments potentially transforming into more flexible or disordered structures like β-turns or 3_{10}-helices. An increase in 3_{10}-helix and β-turn components is often associated with reorganization of hydrogen-bonding patterns and surface exposure of peptide chains. This is consistent with minimal structural denaturation caused by reactive species generated during CP treatment (Misra et al., 2015). These structural changes can therefore have a major impact on functional properties of the protein. At moderate unfolding levels, the increase of β-turn and 3_{10}-helix structures may promote surface flexibility and interfacial activity, which could improve foaming or emulsifying capabilities (Husband et al., 2001; Mune & Sogi, 2016). Consistent of these findings, emulsification and foaming properties of CP-treated proteins were higher than those of the untreated proteins (Table 1). Husband et al. (2001) showed that proteins adsorbed at the oil–water interface had a higher proportion of intermolecular β-turn structures, which is consistent with the observed structural changes in the current study.

Table 3
L*, a*, b* color parameters, ΔE, Chroma, Hue angle, Whiteness index and Browning index values of the untreated control sample and cold plasma-treated protein extracts from *C. prolifera* (obtained under power of 87.50 W, treatment time of 6.63 min and pressure of 90 Pa).

Color parameters	Control	Cold plasma-treated protein
L*	76.99 ± 0.05^{a}	69.94 ± 0.49^{b}
a*	2.74 ± 0.03^{a}	2.23 ± 0.07^{b}
b*	20.32 ± 0.12^{a}	19.93 ± 0.13^{a}
ΔE	0.00 ± 0.00^{b}	2.82 ± 0.09^{a}
Chroma	20.50 ± 0.13^{a}	20.06 ± 0.16^{a}
Hue angle	82.31 ± 0.04^{b}	83.61 ± 0.23^{a}
WI	69.18 ± 0.13^{a}	63.89 ± 0.48^{b}
BI	32.63 ± 0.28^{b}	35.19 ± 0.56^{a}

L*: Brightness/darkness), a*: Redness/greenness), b*: Yellowness/blueness, ΔE: Total color difference, WI: Whiteness index and BI: Browning index. Different lower letters in the same line indicate significant differences between control and cold plasma-treated protein ($p < 0.05$).

The unfolding of protein structures through etching and the oxidation of amino acid groups by active particles during CP treatment are the causes of these changes in secondary structures, which have a direct impact on properties required for solubility, emulsification, and foam formation. Furthermore, the relationship between hydrophobicity and structural elements like α-helices and β-sheets specifically affects solubility and emulsification capacity: a decrease in α-helix content and an increase in β-sheet content typically result in enhanced hydrophobicity, which decreases solubility (M. Li, Peng, et al., 2024). Therefore, in the present study, the increase in WAC and solubility of the CP-treated proteins can be related to the decrease in β-sheet (Table 1). Consequently, a careful balance between structural loosening and functional performance is reflected in the secondary structural transition seen in

Table 4
Amino acid composition (g/hg protein) of cold plasma-treated and untreated protein extracts from *C. prolifera* (obtained under power of 87.50 W, treatment time of 6.63 min and pressure of 90 Pa).

Amino acid	Control	CP-treated protein	FAO/WHO standard mode for children (FAO/WHO, 2007; FAO/WHO, 2013)	FAO/WHO standard mode for adults (FAO/WHO, 2007; FAO/WHO, 2013)
Isoleucine	0.09 ± 0.00[a]	0.08 ± 0.01[a]	2.80	1.30
Leucine	0.31 ± 0.01[a]	0.27 ± 0.03[a]	6.60	1.90
Lysine	0.37 ± 0.11	nd	5.80	1.60
Methionine	nd	nd		
Tyrosine	nd	0.29 ± 0.03		
Phenylalanine	0.26 ± 0.01[a]	0.23 ± 0.02[a]		
Threonine	nd	nd	3.40	0.90
Valine	0.18 ± 0.01[a]	0.05 ± 0.00[b]	3.50	1.30
Histidine	1.00 ± 0.06[a]	0.60 ± 0.00[b]	1.90	1.60
Tryptophan	nd	2.89 ± 0.91	1.10	0.50
EAA	**2.21 ± 0.04[b]**	**4.41 ± 0.20[a]**	**25.1**	**9.1**
Asparagine	0.84 ± 0.01[a]	0.70 ± 0.00[b]		
Glutamic acid	1.16 ± 0.13[a]	0.88 ± 0.00[b]		
Serine	1.10 ± 0.01[a]	1.03 ± 0.07[a]		
Glycine	0.77 ± 0.01[a]	0.55 ± 0.16[a]		
Arginine	0.41 ± 0.00[a]	0.39 ± 0.02[a]		
Alanine	0.74 ± 0.01[a]	0.70 ± 0.11[a]		
NEAA	**5.02 ± 0.03[a]**	**4.95 ± 0.09[a]**		
Total amino acids	**7.23 ± 0.04[a]**	**9.36 ± 0.15[a]**		
AAS (%)	**30.57**	**47.12**		
EAAS (%)	**8.14**	**16.24**		

EAA: Essential amino acids, NEAA: Non-essential amino acids. AAS: Amino acid score, EAAS: Essential amino acid score. FAO: Food and Agriculture Organization. WHO: World Health Organization. Different lower letters in the same line indicate significant differences between control and cold plasma-treated protein ($p < 0.05$).

FT-IR spectra; although substantial denaturation may damage functionality, moderate plasma exposure may improve it.

3.5.2. SEM

The microstructures of untreated and CP-treated proteins were observed using SEM analysis (Fig. 5). According to Fig. 5, there are obvious differences in the microstructures of the proteins between untreated and CP-treated protein extracts prepared under optimum CP treatment conditions. CP-treated proteins had a microstructure that was consistent with a porous and spongy substance and had some cracks on its surface. There were clear indications of severe damage and rupture on the surface of CP-treated proteins. Cracks and porous structure observed in SEM images are consistent with CP-induced protein oxidation because reactive species can break disulfide bonds and change secondary structure in proteins determined by FT-IR analysis, resulting in both chemical and morphological modifications (Eazhumalai, Kalaivendan, & Annapure, 2023). On the other hand, the control showed a compact microstructure with a surface that was comparatively smooth. Cracks and holes in the protein surface could indicate that it was coarse and heterogeneous. Similarly, following atmospheric CP treatment, surface of the soy protein isolate exhibited similar alterations, and its functional characteristics changed (Sharafodin and Soltanizadeh, 2022). Consequently, it is anticipated that ROS and RNS contact will enhance functional characteristics of the proteins. According to Monica et al. (2025), ROS and RNS can etch the surface of proteins and, during the etching process, cleave the C-H and C-C bonds in proteins, which adds to the surface roughness. Moreover, CP-treated proteins were more small particles compared to control. These results are consistent with some studies by conducted Zhang et al. (2022) and Rout and Srivastav, 2024.

3.6. Color attributes

Color is one of the most important parameters of food as it provides the first perception on freshness and safety. Color changes in the CP-treated proteins and the untreated protein extracts are shown in Table 3. Compared to the control, L* and a* values of CP-treated samples decreased significantly after CP application ($p < 0.05$). The untreated sample exhibited a slight increase in lightness compared to the treated sample, which appeared slightly darker ($p < 0.05$). CP treatment of proteins has been reported to have caused mild oxidation of the proteins (Sharma, Prabhakar, & Singh, 2022). Moreover, the isomerization of color pigments bound to proteins may be a reason for color changes after CP treatment (Khodabandeh et al., 2024). On the other hand, b* values of CP-treated samples were found to be closely related to the untreated samples, with no statistically significant difference between them (Table 3). The differences between the CP-treated protein extracts and control can be explained by the color difference (ΔE) and it was calculated as 2.82 ± 0.09 for the treated sample ($p < 0.05$, Table 3). This change can be attributed to the reaction between plasma actives (mainly ROS and RNS) and substances like pigments and proteins (T. Zhang, He, Zhang, & Jiang, 2024). Furthermore, browning index increased, and whiteness index decreased due to augmentation of the brown pigments which occurred after CP treatment (Table 3).

3.7. Nutritional properties

Amino acid composition of CP-treated proteins, the untreated protein extracts and reference values of essential amino acids for children and adults determined by FAO and WHO are presented in Table 4 (FAO/WHO, 2013). A total of 12 and 13 amino acids were detected in the untreated and CP-treated protein extracts, respectively (Table 4). Total amino acid content was 7.23 ± 0.04 and 9.36 ± 0.15 g/hg for untreated and CP-treated protein extract, respectively. On the other hand, as shown in Table 4, the essential amino acid contents of the control and CP-treated proteins were 2.21 ± 0.04 and 4.41 ± 0.20 g/hg, respectively, while the total amino acid contents were 7.23 ± 0.04 and 9.36 ± 0.15 g/hg, respectively. Similarly, in a previous study, untreated total amino acid composition of *Caulerpa lentillifera* was determined as 7.05–12.37 g/hg and essential amino acid ranged from 2.89 to 4.65 g/hg (Zhou et al., 2025). According to the results, the most abundant EAAs in untreated and CP-treated protein extracts were His and Trp, respectively (Table 4). Trp is required for the *in vivo* synthesis of proteins. The treatment of autism, cardiovascular disease, depression, inflammatory bowel disease, multiple sclerosis, sleep, social function, chronic renal disease, cognitive function, and microbial infections may benefit from dietary Trp and its metabolites (Friedman, 2018). Furthermore, in untreated protein extracts, His amino acid content, which plays a variety of functions in tissue growth and repair, histamine production, and protein interaction, was close (1.00 %) to that of FAO/WHO need (1.60%) (FAO/WHO, 2013).

In the present study, amino acid content reduced, excluding Tyr and Trp after CP treatment (Table 4). It is known that CP, which depends on the processing variables (voltage, time, and frequency), can break peptide bonds, oxidize side chains of amino acids, create cross-links across polypeptide chains and change the amino acid content (Rout et al. (2025). Aromatic and sulfurous amino acids, such as cysteine and

methionine, are especially susceptible to oxidation (Sharma & Singh, 2020). Ring cleavages of histidine and tryptophan, nitration/nitrosylation, and the addition of one, two, or three oxygen atoms to aromatic (tyrosine, histidine, and phenylalanine) and neutral amino acids (isoleucine and proline) are the main alterations during CP treatment (Wenske et al., 2020).

Quality of a protein can be evaluated by comparing its amino acid composition to a reference pattern. Nutritional quality of protein is assessed using AAS and the ratio of EAA to TAA (total amino acids). The AAS of control and CP-treated protein extracts was calculated as 30.57 g/hg and 47.12 g/hg, respectively (Table 4). The EAAS of control and CP-treated protein extracts was determined as 8.14 g/hg and 16.24 g/hg, respectively (Table 4). Cold plasma caused an increase in EAAS and AAS.

4. Conclusion

In this study, CP treatment was effectively performed to modify the structure and techno-function of algae-based proteins. The identified optimum conditions (power of 87.50 W, treatment time of 6.63 min and pressure of 90 Pa) also appear mechanistically plausible and RSM-based optimization is statistically valid. In addition to improved antioxidant activity, protein solubility, and water absorption capacity of algae-based protein extracts after CP treatment, reactive species of the plasma caused changes in secondary structure elements, partial denaturation or oxidation of proteins. When the protein extracts obtained under the optimized conditions were evaluated together with their functional properties, antioxidant activity, and FT-IR-confirmed secondary structure changes, the results supported that the optimum processing conditions of CP represents a balance between controlled oxidation and structural preservation for the algal protein extracts. Moderate plasma power and treatment time likely ensured efficient generation of reactive oxygen and nitrogen species without excessive degradation. Similar findings have been reported for bio-derived substrates such as soy and whey proteins treated with CP treatment (Segat et al., 2015; Zhang et al., 2021). On the other hand, particularly regarding contribution of reactive species, the exact mechanisms driving plasma-induced changes are still partially unknown. Therefore, to demonstrate more precise causal links between plasma characteristics and biomolecular reactions, future studies should incorporate controlled parameter optimization and comprehensive plasma treatments. Moreover, sensorial and toxicological properties of algae-based proteins should be investigated to totally determine the performance of CP-treated algae-based proteins in future studies from a holistic perspective before they are added to foods or consumed directly because the usage of algae-based proteins can provide some benefits in terms of sustainability, nutritional value, and development of clean-label foods.

CRediT authorship contribution statement

Aysun Yücetepe: Writing – review & editing, Writing – original draft, Methodology, Investigation, Conceptualization. **Emine Şükran Okudan:** Writing – original draft, Resources, Conceptualization. **Tuba Esatbeyoglu:** Writing – review & editing, Supervision, Project administration, Conceptualization.

Declaration of competing interest

The authors declare that they have no known competing financial interests or personal relationships that could have appeared to influence the work reported in this paper.

Acknowledgments

This study was supported by The Scientific and Technological Research Council of Turkey (TUBITAK) (TUBITAK 2219 Project-International Postdoctoral Research Fellowship Program). We would like to thank TUBITAK for this valuable support. Moreover, we would like to thank to Prof. Armin Feldhoff and Mr. Frank Steinbach from the Institute of Physical Chemistry and Electrochemistry, Leibniz University Hannover for their helping in SEM analysis. Also, we thank to Ms. Mona Grünwald for her helping in HPLC analysis. The authors declare that grammar and language correction tools were used to enhance the readability of the article. The publication of this article was funded by the Open Access Fund of Leibniz Universität Hannover.

Appendix A. Supplementary data

Supplementary data to this article can be found online at https://doi.org/10.1016/j.lwt.2025.118840.

Data availability

Data will be made available on request.

References

Aboul-enein, Y., Bunacıu, A., & Fleschın, S. (2014). Evaluation of the protein secondary structures using Fourier transform infrared spectroscopy. *Gazi University Journal of Science, 27*(1), 637–644.

Akgün, D., Gültekin-Özgüven, M., Yücetepe, A., Altin, G., Gibis, M., Weiss, J., & Özçelik, B. (2020). Stirred-type yoghurt incorporated with sour cherry extract in chitosan-coated liposomes. *Food Hydrocolloids, 101*, Article 105532. https://doi.org/10.1016/j.foodhyd.2019.105532

Andrade, J., Pereira, C. G., de Almeida Junior, J. C., Viana, C. C. R., de Oliveira Neves, L. N., da Silva, P. H. F., … dos Anjos, V. D. C. (2019). FTIR-ATR determination of protein content to evaluate whey protein concentrate adulteration. *LWT, 99*, 166–172.

Apak, R., Güçlü, K., Özyürek, M., & Karademir, S. E. (2004). Novel total antioxidant capacity index for dietary polyphenols and vitamins C and E, using their cupric ion reducing capability in the presence of neocuproine: CUPRAC method. *Journal of Agricultural and Food Chemistry, 52*(26), 7970–7981.

Apelqvist, J., Robson, A., Helmke, A., Rousseau, A., Boekema, B., den Braber, E., Szili, E., Sturmer, E., Bockmann, L., & Gaur, N. (2024). Cold plasma: An emerging technology for clinical use in wound healing. *Journal of Wound Management, 25*(3), 1–84.

Barbhuiya, R.I., Singha, P., & Singh, S.K. (2021). A comprehensive review on impact of non-thermal processing on the structural changes of food components. *Food Research International*, *149*, Article 110647, doi:10.1016/j.foodres.2021.110647.

Basak, S., & Annapure, U. S. (2022). Recent trends in the application of cold plasma for the modification of plant proteins-A review. *Future Foods, 5*, Article 100119.

Bußler, S., Steins, V., Ehlbeck, J., & Schlüter, O. (2015). Impact of thermal treatment versus cold atmospheric plasma processing on the techno-functional protein properties from *Pisum sativum* 'Salamanca'. *Journal of Food Engineering, 167*, 166–174.

Charlton, N. C., Mastyugin, M., Török, B., & Török, M. (2023). Structural features of small molecule antioxidants and strategic modifications to improve potential bioactivity. *Molecules, 28*(3), 1057.

Chen, Y., Chen, J., Chang, C., Chen, J., Cao, F., Zhao, J., & Zhu, J. (2019). Physicochemical and functional properties of proteins extracted from three microalgal species. *Food Hydrocolloids, 96*, 510–517.

Chen, Y.-Q., Cheng, J.-H., & Sun, D.-W. (2020). Chemical, physical and physiological quality attributes of fruit and vegetables induced by cold plasma treatment: Mechanisms and application advances. *Critical Reviews in Food Science and Nutrition, 60*(16), 2676–2690.

Dai, Z., Wu, Z., Jia, S., & Wu, G. (2014). Analysis of amino acid composition in proteins of animal tissues and foods as pre-column o-phthaldialdehyde derivatives by HPLC with fluorescence detection. *Journal of Chromatography B, 964*, 116–127.

De Meutter, J., & Goormaghtigh, E. (2021). Evaluation of protein secondary structure from FTIR spectra improved after partial deuteration. *European Biophysics Journal, 50*(3–4), 613–628.

Dubey, S. K., Parab, S., Alexander, A., Agrawal, M., Achalla, V. P. K., Pal, U. N., Pandey, M. M., & Kesharwani, P. (2022). Cold atmospheric plasma therapy in wound healing. *Process Biochemistry, 112*, 112–123.

Eazhumalai, G., Kalaivendan, R. G. T., & Annapure, U. S. (2023). Effect of atmospheric pin-to-plate cold plasma on oat protein: Structural, chemical, and foaming characteristics. *International Journal of Biological Macromolecules, 242*, Article 125103.

Escobar Cano, G., Wellmann, M., Steinbach, F., Thiem, M., Xie, W., Weidenkaff, A., & Feldhoff, A. (2024). Enhanced performance of La2NiO4+ δ oxygen-transporting membranes using crystal facet engineering via microemulsion-based synthesis. *Chemistry of Materials, 36*(19), 9557–9574.

FAO/WHO. (2007). Protein and amino acid requirements in human nutrition. In *World Health Organization technical report series 935*. https://www.fao.org/.

FAO/WHO. (2013). Dietary protein quality evaluation in human nutrition: Report of an FAO expert consultation. *FAO Food & Nutrition Paper, 92*. https://www.fao.org/.

Friedman, M. (2018). Analysis, nutrition, and health benefits of tryptophan. *International Journal of Tryptophan Research, 11*, Article 1178646918802282.
Gani, A., ul Ashraf, Z., Noor, N., & Wani, I. A. (2022). Ultrasonication as an innovative approach to tailor the apple seed proteins into nanosize: Effect on protein structural and functional properties. *Ultrasonics Sonochemistry, 86*, Article 106010.
Gavahian, M., Chu, Y.-H., Khaneghah, A. M., Barba, F. J., & Misra, N. N. (2018). A critical analysis of the cold plasma induced lipid oxidation in foods. *Trends in Food Science & Technology, 77*, 32–41.
Gómez-Ordóñez, E., & Rupérez, P. (2011). FTIR-ATR spectroscopy as a tool for polysaccharide identification in edible brown and red seaweeds. *Food Hydrocolloids, 25*(6), 1514–1520.
Han, X., Mi, Y., Ji, Y., Sun, M., Tang, H., Dong, F., & Guo, Z. (2024). A novel chitosan antioxidant bearing sulfhydryl group: Synthesis, characterization and activity assessment. *International Journal of Biological Macromolecules, 261*, Article 129816.
Hara, H., & Adachi, T. (2021). Molecular mechanisms of non-thermal atmospheric pressure plasma-induced cellular responses. *Japanese Journal of Applied Physics, 60*(2), Article 020501.
Huang, C., Feng, W., Xiong, J., Wang, T., Wang, W., Wang, C., & Yang, F. (2019). Impact of drying method on the nutritional value of the edible insect protein from black soldier fly (*Hermetia illucens* L.) larvae: amino acid composition, nutritional value evaluation, *in vitro* digestibility, and thermal properties. *European Food Research and Technology, 245*(1), 11–21.
Husband, F. A., Garrood, M. J., Mackie, A. R., Burnett, G. R., & Wilde, P. J. (2001). Adsorbed protein secondary and tertiary structures by circular dichroism and infrared spectroscopy with refractive index matched emulsions. *Journal of Agricultural and Food Chemistry, 49*(2), 859–866.
Ji, H., Dong, S., Han, F., Li, Y., Chen, G., Li, L., & Chen, Y. (2018). Effects of dielectric barrier discharge (DBD) cold plasma treatment on physicochemical and functional properties of peanut protein. *Food and Bioprocess Technology, 11*(2), 344–354. https://doi.org/10.1007/s11947-017-2015-z
Ji, H., Han, F., Peng, S., Yu, J., Li, L., Liu, Y., … Chen, Y. (2019). Behavioral solubilization of peanut protein isolate by atmospheric pressure cold plasma (ACP) treatment. *Food and Bioprocess Technology, 12*, 2018–2027.
Jiang, Y. I., Li, D., Tu, J., Zhong, Y., Zhang, D., Wang, Z., & Tao, X. (2021). Mechanisms of change in gel water-holding capacity of myofibrillar proteins affected by lipid oxidation: The role of protein unfolding and cross-linking. *Food Chemistry, 344*, Article 128587.
Kashfi, A.S., Ramezan, Y., & Khani, M.R. (2020). Simultaneous study of the antioxidant activity, microbial decontamination and color of dried peppermint (*Mentha piperita* L.) using low pressure cold plasma. *LWT*, *123*, Article 109121,10.1016/j.lwt.2020.109121.
Kemal, M., Teka, T.A., Dibaba, K., & Urugo, M.M. (2025). Effects of processing methods on nutrient and antinutrient composition, techno-functional and antioxidant properties of mungbean (*Vigna radiata* (L.) R. Wilczek) varieties. *LWT*, *222*, Article 117663,10.1016/j.lwt.2025.117663.
Khodabandeh, M., Azizi, M., Shokri, B., Bahreini, M., Rezadoost, H., & Salehi, M. (2024). Optimization of the radiofrequency low-pressure cold plasma conditions for decontamination of saffrons. *Food and Bioprocess Technology, 17*(1), 271–297.
Kong, J., & Yu, S. (2007). Fourier transform infrared spectroscopic analysis of protein secondary structures. *Acta Biochimica et Biophysica Sinica, 39*, 549–559.
Kumar, A., Nayak, R., Purohit, S.R., & Rao, P.S. (2021). Impact of UV-C irradiation on solubility of Osborne protein fractions in wheat flour. *Food Hydrocolloids*, *110*, Article 105845,10.1016/j.foodhyd.2020.105845.
Lambrecht, M. A., Deleu, L. J., Rombouts, I., & Delcour, J. A. (2018). Heat-induced network formation between proteins of different sources in model systems, wheat-based noodles and pound cakes. *Food Hydrocolloids, 79*, 352–370.
Langendörfer, L. J., Avdylaj, B., Hensel, O., & Diakité, M. (2023). Design of plant-based food: Influences of macronutrients and amino acid composition on the techno-functional properties of legume proteins. *Foods, 12*(20), 3787.
Laroque, D. A., Seó, S. T., Valencia, G. A., Laurindo, J. B., & Carciofi, B. A. M. (2022). Cold plasma in food processing: Design, mechanisms, and application. *Journal of Food Engineering, 312*, Article 110748.
Laroussi, M. (2020). Cold plasma in medicine and healthcare: The new frontier in low temperature plasma applications. *Frontiers in Physics, 8*, 74.
Li, X., Li, M., Ji, N., Jin, P., Zhang, J., Zheng, Y., Zhang, X., & Li, F. (2019). Cold plasma treatment induces phenolic accumulation and enhances antioxidant activity in fresh-cut pitaya (*Hylocereus undatus*) fruit. *LWT*, *115*, Article 108447,10.1016/j.lwt.2019.108447.
Li, B., Peng, L., Cao, Y., Liu, S., Zhu, Y., Dou, J., Yang, Z., & Zhou, C. (2024). Insights into cold plasma treatment on the cereal and legume proteins modification: Principle, mechanism, and application. *Foods, 13*(10), 1522.
Li, M., Wang, X., Shi, T., Xiong, Z., Jin, W., Bao, Y., Monto, A.R., Yuan, L., & Gao, R. (2024). Mechanism of plasma-activated water promoting the heat-induced aggregation of myofibrillar protein from silver carp (*Aristichthys nobilis*). *Innovative Food Science & Emerging Technologies*, *91*, Article 103555,10.1016/j.ifset.2023.103555.
Liu, J. J., Gasmalla, M. A. A., Li, P., & Yang, R. (2016). Enzyme-assisted extraction processing from oilseeds: Principle, processing and application. *Innovative Food Science & Emerging Technologies, 35*, 184–193.
Lyu, S., Chen, M., Wang, Y., Zhang, D., Zhao, S., Liu, J., Pan, F., & Zhang, T. (2023). Foaming properties of egg white proteins improved by enzymatic hydrolysis: The changes in structure and physicochemical properties. *Food Hydrocolloids*, *141*, Article 108681,10.1016/j.foodhyd.2023.108681.
Mehr, H. M., & Koocheki, A. (2020). Effect of atmospheric cold plasma on structure, interfacial and emulsifying properties of Grass pea (*Lathyrus sativus* L.) protein isolate. *Food Hydrocolloids, 106*, Article 105899.
Metelmann, H.-R., Seebauer, C., Miller, V., Fridman, A., Bauer, G., Graves, D. B., Pouvesle, J.-M., Rutkowski, R., Schuster, M., & Bekeschus, S. (2018). Clinical experience with cold plasma in the treatment of locally advanced head and neck cancer. *Clinical Plasma Medicine, 9*, 6–13.
Misra, N. N., Kaur, S., Tiwari, B. K., Kaur, A., Singh, N., & Cullen, P. J. (2015). Atmospheric pressure cold plasma (ACP) treatment of wheat flour. *Food Hydrocolloids, 44*, 115–121.
Misra, N. N., & Roopesh, M. S. (2019). Cold plasma for sustainable food production and processing. In F. Chemat, & M. Vian (Eds.), *Green food processing techniques* (pp. 431–453). London: Academic Press.
Monica, V., Anbarasan, R., & Mahendran, R. (2025). Cold plasma-induced changes in the structural and techno-functional properties of sprouted foxtail millet protein concentrate. *Food and Bioprocess Technology, 18*(1), 850–867.
Mune, M. A. M., & Sogi, D. S. (2016). Emulsifying and foaming properties of protein concentrates prepared from cowpea and bambara bean using different drying methods. *International Journal of Food Properties, 19*(2), 371–384.
Onyenweaku, E.O., Akah, L.U., Kesa, H., Alawa, D.A., Ebai, P.A., Kalu, U.U., … Owan, V. J. (2022). Protein quality evaluation of some commonly consumed bird egg varieties using amino acid scores. *Biochemistry Research International*, *2022*(1), Article 6536826, doi: 10.1155/2022/6536826.
Pérez-Andrés, J.M., Álvarez, C., Cullen, P.J., & Tiwari, B.K. (2019). Effect of cold plasma on the techno-functional properties of animal protein food ingredients. *Innovative Food Science & Emerging Technologies*, *58*, Article 102205,10.1016/j.ifset.2019.102205.
Perner, J., & Matoušek, J. (2024). Cold plasma treatment influences the physiological parameters of millet. *Photosynthetica, 62*(1), 126.
Roshanfekr, A., Moeini, Z., Golmohammadi, F., Balalaie, S., & Seyedarabi, A. (2025). Antioxidative effects of phytoaromatic compounds on the cysteine of the SKCGS peptide as a critical aggregation domain of tau. *Scientific Reports*, *15*(1), Article 23206,doi: 10.1038/s41598-025-04999-x.
Rout, S., Panda, P. K., Dash, P., Srivastav, P. P., & Hsieh, C. T. (2025). Cold plasma-induced modulation of protein and lipid macromolecules: A review. *International Journal of Molecular Sciences, 26*(4), 1564.
Sanjeewa, K.A., Herath, K.H.I.N.M., Kim, Y.S., Jeon, Y.J., & Kim, S.K. (2023). Enzyme-assisted extraction of bioactive compounds from seaweeds and microalgae. *TrAC, Trends in Analytical Chemistry*, *167*, Article 117266,10.1016/j.trac.2023.117266.
Rout, S., & Srivastav, P. P. (2024). Modification of soy protein isolate and pea protein isolate by high voltage dielectric barrier discharge (DBD) atmospheric cold plasma: Comparative study on structural, rheological and techno-functional characteristics. *Food Chemistry, 447*, Article 138914.
Segat, A., Misra, N. N., Cullen, P. J., & Innocente, N. (2015). Atmospheric pressure cold plasma (ACP) treatment of whey protein isolate model solution. *Innovative Food Science & Emerging Technologies, 29*, 247–254.
Sensu, E., Ayar, E. N., Okudan, E. S., Ozcelik, B., & Yucetepe, A. (2023). Characterization of proteins extracted from *Ulva* sp., *Padina* sp., and *Laurencia* sp. macroalgae using green technology: Effect of in vitro digestion on antioxidant and ACE-I inhibitory activity. *ACS Omega, 8*(51), 48689–48703.
Sharafodin, H., & Soltanizadeh, N. (2022). Potential application of DBD Plasma Technique for modifying structural and physicochemical properties of soy protein ısolate. *Food Hydrocolloids, 122*, Article 107077.
Sharifian, A., Soltanizadeh, N., & Abbaszadeh, R. (2019). Effects of dielectric barrier discharge plasma on the physicochemical and functional properties of myofibrillar proteins. *Innovative Food Science & Emerging Technologies, 54*, 1–8.
Sharma, S., Prabhakar, H., & Singh, R. K. (2022). Atmospheric cold plasma-induced changes in milk proteins. *Food and Bioprocess Technology, 15*(12), 2737–2748.
Sharma, S., & Singh, R.k. (2020). Cold plasma treatment of dairy proteins in relation to functionality enhancement. *Trends in Food Science & Technology, 102*, 30–36.
Shen, L., Wang, X., Wang, Z., Wu, Y., & Chen, J. (2008). Studies on tea protein extraction using alkaline and enzyme methods. *Food Chemistry, 107*(2), 929–938.
Smith, P. E., Krohn, R. I., Hermanson, G. T., Mallia, A. K., Gartner, F. H., Provenzano, M., … Klenk, D. C. (1985). Measurement of protein using bicinchoninic acid. *Analytical Biochemistry, 150*(1), 76–85.
Wang, X., Chao, H., Ma, W., Li, Y., Yang, H., Chen, W., & Li, L. (2025). Preservation mechanism of cold plasma pretreatment on the antioxidant activity and quality of prune during storage. *Food Research International*, *206*, Article 116081,10.1016/j.foodres.2025.116081.
Wang, X.Y., Han, Z.T., Dong, Z.Y., Zhang, T.H., Duan, J.W., Ai, L., & Xu, Y.Y. (2024). Atmospheric-pressure cold plasma-assisted enzymatic extraction of high-temperature soybean meal proteins and effects on protein structural and functional properties. *Innovative Food Science & Emerging Technologies*, *92*, Article 103586,10.1016/j.ifset.2024.103586.
Wang, P., Wang, Y., Du, J., Han, C., & Yu, D. (2024). Effect of cold plasma treatment of sunflower seed protein modification on its structural and functional properties and its mechanism. *Food Hydrocolloids*, *155*, Article 110175,10.1016/j.foodhyd.2024.110175.
Wang, W., Yang, P., Rao, L., Zhao, L., Wu, X., Wang, Y., & Liao, X. (2022). Effect of high hydrostatic pressure processing on the structure, functionality, and nutritional properties of food proteins: A review. *Comprehensive Reviews in Food Science and Food Safety, 21*(6), 4640–4682.
Wei, S., Zhao, L., Liu, Z., Zhang, X., Hui, Y., Wang, D., Liu, Z., & Liu, G. (2023). Cold plasma treatment for Astragalus membranaceus seed germination and seedling growth improvement. *Legume Research-An International Journal, 46*(5), 609–615.
Wenske, S., Lackmann, J.-W., Bekeschus, S., Weltmann, K.-D., Von Woedtke, T., & Wende, K. (2020). Nonenzymatic post-translational modifications in peptides by cold plasma-derived reactive oxygen and nitrogen species. *Biointerphases, 15*(6).

Withana-Gamage, T. S., Wanasundara, J. P., Pietrasik, Z., & Shand, P. J. (2011). Physicochemical, thermal and functional characterisation of protein isolates from Kabuli and Desi chickpea (Cicer arietinum L.): A comparative study with soy (*Glycine max*) and pea (*Pisum sativum* L.). *Journal of the Science of Food and Agriculture, 91*(6), 1022–1031.

Yu, J. J., Chen, G. Y., Zhang, Y. F., Zheng, X. C., Jiang, P. Y., Ji, H., … Chen, Y. (2021). Enhanced hydration properties and antioxidant activity of peanut protein by covalently binding with sesbania gum via cold plasma treatment. *Innovative Food Science & Emerging Technologies, 68*, Article 102632.

Yu, J., Zhang, Z., Lin, X., Ji, Y., Zhang, R., Ji, H., & Chen, Y. (2023). Changes in the structure and hydration properties of high-temperature peanut protein induced by cold plasma oxidation. *International Journal of Biological Macromolecules, 253*, Article 127500.

Yucetepe, A., Okudan, E.Ş., & Özçelik, B. (2022). Antioxidant activity and techno-functional properties of protein extracts from *Caulerpa prolifera*: Optimization of enzyme-assisted extraction by response surface methodology. *Journal of Food and Nutrition Research, 61*(3).

Zhang, Q., Cheng, Z., Zhang, J., Nasiru, M. M., Wang, Y., & Fu, L. (2020). Atmospheric cold plasma treatment of soybean protein isolate: Insights into the structural, physicochemical, and allergenic characteristics. *Journal of Food Science, 86*(1), 68–77. https://doi.org/10.1111/1750-3841.15556

Zhang, Q., Cheng, Z., Zhang, J., Nasiru, M. M., Wang, Y., & Fu, L. (2021). Atmospheric cold plasma treatment of soybean protein isolate: Insights into the structural, physicochemical, and allergenic characteristics. *Journal of Food Science, 86*(1), 68–77.

Zhang, T., He, L., Zhang, M., & Jiang, H. (2024). Physicochemical characterization and sensory enhancement of cold plasma treated black whole wheat flour. *Scientific Reports*, *14*(1), Article 24366,doi: 10.1038/s41598-024-71978-z.

Zhang, N., Hu, Y., An, L., Li, Q., Yin, J., Li, J., … Yan, C.H. (2022). Surface activation and Ni-S stabilization in NiO/NiS2 for efficient oxygen evolution reaction. *Angewandte Chemie*, *134*(35), Article e202207217,10.1002/ange.202207217.

Zhou, W., Wang, Y., Xu, R., Tian, J., Li, T., & Chen, S. (2025). Comparative analysis of the nutrient composition of *Caulerpa lentillifera* from various cultivation sites. *Foods, 14*(3), 474.